Chemical Engineering Journal 404 (2021) 126503

Contents lists available at ScienceDirect

Chemical Engineering Journal

journal homepage: www.elsevier.com/locate/cej

CO_2 absorption rate in biphasic solvent of aminoethylethanolamine and diethylethanolamine

Fei Liu[a,b], Gary T. Rochelle[b,*], Tao Wang[a,*], Eric Chen[b], Mengxiang Fang[a]

[a] State Key Laboratory of Clean Energy Utilization, Zhejiang University, Hangzhou 310027, China
[b] McKetta Department of Chemical Engineering, The University of Texas at Austin, 200 E Dean Keeton St., Austin, TX 78712, USA

HIGHLIGHTS

- 25% AEEA/50% DEEA forms organic and aqueous phases at P_{CO2}* greater than 100 Pa.
- The organic phase absorbs CO_2 2–7 times faster than aqueous phase.
- Instantaneous reaction model was built to explain the fast rate of organic phase.
- CO_2 capacity of aqueous phase is 2–10 times greater than organic phase.
- Biphasic solvent of AEEA/DEEA is superior to 30% MEA and competitive with 30% PZ.

ARTICLE INFO

Keywords:
Absorption rate
Biphasic solvent
Mass transfer coefficient
Physical solubility
Viscosity

ABSTRACT

Amine scrubbing is currently the most promising technology for CO_2 capture from gas turbine and coal-fired flue gas. It is hindered by high regeneration energy and high capital cost. Biphasic solvent of 25% aminoethylethanolamine (AEEA)/50% diethylethanolamine (DEEA) could be a potential solution as it may achieve significant reduction in regeneration energy. A fast CO_2 absorption rate is preferred to reduce the capital cost of the absorber. In this work, the CO_2 absorption rate (k_g') of the biphasic solvent was measured in a wetted wall column at 40 °C and at the loading conditions in the absorber. At CO_2 equilibrium partial pressure (P_{CO2}*) lower than 100 Pa, 25% AEEA/50% DEEA is homogeneous. The CO_2 absorption rate, k_g', is as fast as 30% PZ (3 times faster than 30% MEA). When P_{CO2}* is greater than 100 Pa, 25% AEEA/50% DEEA forms aqueous and organic phases after CO_2 absorption. It was first found that the organic phase of 25% AEEA/50% DEEA absorbs CO_2 2–7 times faster than the aqueous phase because of greater physical CO_2 solubility at the same P_{CO2}* and physical mass transfer coefficient. The k_g' of the organic phase is much faster than 30% MEA and 25% AEEA at lean and rich loading and even greater than 30% PZ at lean loading. The instantaneous reaction mechanism fits the kinetics of CO_2 absorption in the organic phase at low P_{CO2}*. The slow k_g' of the aqueous phase results from greater viscosity which significantly reduces the physical mass transfer coefficient. The CO_2 capacity of the aqueous phase is 2.9 times, 1.8 times, and 5.3 times greater than that of 30% MEA, 30% PZ, and the organic phase, respectively.

1. Introduction

CO_2 capture and storage (CCS) is an effective strategy to mitigate the greenhouse effect by reducing global cumulative CO_2 emissions. Amine scrubbing is currently the most mature technology for CO_2 capture from large stationary sources, such as coal-fired power plants [1]. Aqueous monoethanolamine (MEA, 30 wt%) is the benchmark solvent for this technology [2], but it is challenged by high capital cost and intensive energy consumption [3]. The CO_2 absorption rate and CO_2 capacity of a solvent are two important parameters that determine the capital cost and energy penalty. A faster absorption rate reduces the size of the absorber for the same CO_2 removal efficiency [4]. A higher CO_2 capacity reduces the amount of solvent, which reduces the required heat of solvent regeneration [5]. Various studies [6,7] of alternative amines and blends have been conducted to improve the performance of a solvent by providing high CO_2 capacity, low regeneration heat, and faster absorption rate.

Biphasic solvent is a promising solvent for CO_2 capture as it exhibits

* Corresponding authors.
E-mail addresses: gtr@che.utexas.edu (G.T. Rochelle), oatgnaw@zju.edu.cn (T. Wang).

https://doi.org/10.1016/j.cej.2020.126503
Received 17 June 2020; Received in revised form 25 July 2020; Accepted 29 July 2020
Available online 02 August 2020
1385-8947/

larger CO_2 capacity and may significantly reduce the regeneration energy [8]. A unique feature of the biphasic solvent is that two liquid phases are formed after CO_2 absorption. The aqueous phase is rich in CO_2 and the organic phase is very lean in CO_2. Sending only the aqueous phase to the stripper may improve CO_2 capacity and reduce the sensible heat requirement.

Several amine blends have been identified as biphasic solvents with large CO_2 capacity and low regeneration energy. Zhang et al. [9,10] proposed 3 M N, N-dimethylcyclohexylamine (DMCA)/1 M dipropylamine (DPA) with an optimized CO_2 capacity of 2.3 mol/kg and a regeneration energy of 2.5 GJ/tCO_2. Pinto et al. [11,12] developed 5 M diethylethanolamine (DEEA)/2 M 3-(methylamino)propylamine (MAPA) with a CO_2 capacity of 2 mol/kg and a regeneration energy of 2.2–2.4 GJ/tCO_2. Ciftja et al. [13] analyzed amine species of 5 M DEEA/2 M MAPA at rich loading using a NMR method. Xu et al. [14] studied 4 M DEEA/2 M 1,4-butanediamine (BDA) and measured individual amine distribution in the upper and lower phases by ion chromatography (IC). The CO_2 capacity was 2.2 mol/kg but the regeneration energy was not estimated. Liu et al. [15] evaluated the biphasic behavior of 4.3 M DEEA/2.4 M 2-((2-aminoethyl) amino) ethanol (AEEA), and a high CO_2 capacity of 2.3 mol/kg and a low regeneration energy of 2.2 GJ/tCO_2 was estimated. Zhang et al. [16] evaluated 3 M DMCA/1 M triethylenetetramine (TETA) and the regeneration energy was as low as 2.07 GJ/tCO_2 at the optimal ratio of CO_2-rich phase. Lv et al. [17] proposed 0.5 M diethylene-triamine (DETA)/1.5 M 2-amino-2-methyl-1-propanol (AMP)/3 M pentamethyldiethylenatriamine (PMDETA) with the lowest regeneration energy of 1.83 GJ/tCO_2.

CO_2 absorption rate is another critical criterion for a biphasic solvent to be selected for CO_2 capture. Several studies have measured CO_2 absorption into biphasic solvents. Lv et al. [17] used a double-stirred cell to measure the CO_2 absorption kinetics in unloaded 0.5 M DETA/1.5 M AMP/3 M PMDETA and the overall kinetic reaction rate (k_{ov}) was 2586 s^{-1} at 40 °C, which is 25 times slower than 5 M MEA (65000 s^{-1}) [18]. Wang et al. [19] measured CO_2 absorption rates of N,N-dimethylbutylamine (DMBA)/DEEA in a wetted wall column and the absorption rates of 4 M DMBA/2 M DEEA and 2 M DMBA/4 M DEEA were 2–4 times lower than that of 5 M MEA. The slow CO_2 absorption rate is mainly due to the extremely slow kinetic rate of tertiary amines such as DEEA, PMDETA and DMBA. For example, Ewelina et al. [20] measured the kinetics of CO_2 absorption in DEEA and the kinetic rate constant is 0.13 m^3 mol^{-1} s^{-1} at 40 °C which is two orders of magnitude less than that of 5 M MEA (13 m^3 mol^{-1} s^{-1}).

Diamines such as piperazine (PZ) [7], BDA [21], MAPA [22], AEEA [6] , and DETA [23] exhibited much faster kinetics than MEA and these diamines can increase the CO_2 absorption rate significantly. For example, Xu et al. [21] measured CO_2 absorption rate in unloaded 4 M DEEA/2 M BDA using a wetted wall column and the absorption rate (k_g') was 12% faster than 5 M MEA at 40 °C. Monteiro et al. [24] and Liebenthal et al. [25] used a string of discs to measure unloaded DEEA/MAPA and the pseudo-first order kinetic rate of 5 M DEEA/2 M MAPA is 20 times faster than that of 5 M MEA at 40 °C. Kierzkowska-Pawlak [26] studied the CO_2 absorption in DEEA/AEEA using a stirred-cell reactor and the overall kinetic reaction rate (k_{ov}) was increased by 15 times with 0.3 M AEEA as additive.

CO_2 absorption in the absorber is mostly at rich loading, giving CO_2 equilibrium partial pressure (P_{CO2}*) of 0.5–5 kPa for coal flue gas and 0.1–1 kPa for gas turbine flue gas at 40 °C [27]. CO_2 loading reduces the CO_2 absorption rate of biphasic solvent. Zhang et al. [16] studied 3 M DMCA/1 M TETA in a double-stirred cell and the absorption rate at 0.25 and 0.75 mol CO_2/mol amine was 8% and 16% slower than in 5 M MEA. Wang et al. [28] studied 4 M DEEA/1 M DETA with CO_2 loading of 1.31 mol/L in a wetted wall column at 40 °C and the absorption rate was 2.2 times lower than that of 5 M MEA.

NMR spectroscopy of CO_2 loaded biphasic solvent indicates that speciation in the two phases varies greatly. For example, 25% AEEA/50% DEEA forms two phases at CO_2 loading of 1 mol/kg solution [29]. The composition of the aqueous phase is 42% AEEA, 10% DEEA, and 48% water with 2.3 mol CO_2/kg solution. The organic phase is 11% AEEA, 81% DEEA, and 8% water with 0.1 mol CO_2/kg solution. However, the CO_2 absorption rate of the aqueous and organic phases was not investigated.

Biphasic solvent of 25% AEEA/50% DEEA could be a potential solution for CO_2 capture as it can achieve significant reduction in regeneration energy and may have fast CO_2 absorption rate. This work is to find out the CO_2 absorption behavior of the biphasic solvent after two phases are formed. In this work, the CO_2 absorption rate (k_g') was measured using a wetted wall column (WWC) with a CO_2 loading range giving a CO_2 equilibrium partial pressure (P_{CO2}*) of 0.1–5 kPa at 40 °C. The WWC measurement also provides the equilibrium CO_2 partial pressure for each solvent composition. Measurements were completed with 25% AEEA, 50% DEEA, and AEEA/DEEA blends, and with the aqueous and the organic phases after two phases are formed.

2. Materials and methods

2.1. Materials

The chemicals used in this work are listed in Table 1. Amine solution was prepared by mixing amines and water gravimetrically to achieve the desired concentration. CO_2-loaded solutions were prepared by gravimetrically sparging CO_2 into unloaded amine solutions.

Aqueous 25% AEEA/50% DEEA was used as the biphasic solvent. A previous study [29] indicated that this blend exhibits two phases (aqueous phase and organic phase) when loaded with CO_2. The species composition at 40 °C is shown in Table 2. The CO_2 absorption rates of the aqueous and organic phases were measured at 40 °C in this work.

2.2. Wetted wall column

The CO_2 absorption rate and CO_2 solubility in aqueous amine were measured in a wetted wall column (WWC) coupled with a Fourier Transform Infrared (FTIR) gas analyzer (Gasmet CX4000). The method is the same as that used by Chen and Rochelle [30], Li et al. [31], Du et al. [32], and Yuan and Rochelle [33] except that the FTIR has been substituted for an IR analyzer.

As shown in Fig. 1, CO_2 was mixed with nitrogen using a mass flow controller to the desired concentration. The total gas flow rate (Q_{gas}) was 5 standard L/min. The gas mixture was first saturated with water, then fed to the WWC at 36 to 38 °C. The inlet gas with CO_2 from 1000 to 10,000 ppmv was measured by the FTIR after bypassing the WWC reactor. The total pressure (P_{total}) in the WWC was fixed at 20 psig. CO_2, amine, and water in the outlet gas were measured continuously using the FTIR. Before the FTIR analyzer, the outlet gas was kept at 180 °C using a heated line to prevent amine and water condensation.

About 1.5 L of amine solution loaded with CO_2 was placed in the solvent tank. The solvent was pumped into the WWC at a constant flow rate (Q_{liquid}) of 250 ml/min. The solvent flowed through the inner cell, formed a liquid film in the outer wall, and then was recycled back to the solvent tank. The solvent counter-currently contacts with the gas phase at the surface of the outer wall with the area of 38 cm^2. The temperature of the WWC reactor and solvent was controlled at 40 °C using an oil

Table 1
Chemicals and gases used in this work.

Chemical or gas	CAS number	Purity (%)	Supplier
2-((2-aminoethyl) amino) ethanol (AEEA)	111-41-1	99	Aldrich
2-(Diethylamino)ethanol (DEEA)	100-37-8	99.5	Aldrich
Carbon dioxide (CO_2)	124-38-9	99.99	Praxair
Nitrogen (N_2)	7727-37-9	99.995	Praxair

Table 2
Species composition of the two phases of AEEA/DEEA biphasic solvent at 40 °C [29].

Total CO_2 (mol/kg)[a]	Phase	AEEA (wt %)	DEEA (wt %) [a]	H_2O (wt %)	CO_2 (mol/kg) [a]
1.10	Aqueous phase 1	42	12	46	2.59
	Organic phase 1	10	81	9	0.13
1.47	Aqueous phase 2	42	15	43	3.18
	Organic phase 2	4	87	9	0.08
2.00	Aqueous phase 3	41	18	41	4.08
	Organic phase 3	2	92	6	0.08

[a] mol CO_2/kg (amine + H_2O).

bath. Three thermocouples were used to measure the temperature of the inlet solvent, outlet solvent, and the inlet gas.

2.3. Mass transfer coefficient

The CO_2 absorption flux (N_{Flux}) in the WWC was obtained by Eq. (1).

$$N_{Flux} = \frac{(c_{in} - c_{out})\cdot Q_{gas}}{V_M \cdot A} \quad (1)$$

c_{in} and c_{out} is CO_2 concentration of the inlet and outlet gas of the WWC. Q_{gas} is the total gas flow rate which is 5 L/min in this work. V_M is the ideal gas molar volume at standard temperature and pressure, 22.4 L/mol. A is the gas–liquid contact area of the WWC. The total mass transfer coefficient (K_G) can be calculated using the flux (N_{Flux}) and the driving force (P_d) by Eq. (2). The driving force is the logarithmic mean value of the inlet and outlet CO_2 partial pressures, shown as Eq. (3).

$$K_G = \frac{N_{Flux}}{P_d} \quad (2)$$

$$P_d = \frac{(P_{in} - P^*) - (P_{out} - P^*)}{\ln(\frac{P_{in} - P^*}{P_{out} - P^*})} \quad (3)$$

P_{in} and P_{out} are CO_2 partial pressure in the inlet and outlet gas. The CO_2 concentration in the inlet gas was varied from 1000 to 10000 ppm to minimize the measurement error. Measurement of CO_2 absorption into aqueous piperazine (PZ, 30%) was conducted to verify the experimental method. Fig. 2 shows the CO_2 absorption flux plotted against the driving force using the WWC. When the CO_2 partial pressure is greater than the equilibrium partial pressure of the PZ solvent, the driving force is positive and CO_2 is absorbed into the solvent. When the CO_2 partial pressure is less than the equilibrium partial pressure of the PZ solvent, the driving force is negative and CO_2 is desorbed from the solvent. The slope of the line represents the K_G for CO_2 absorption in

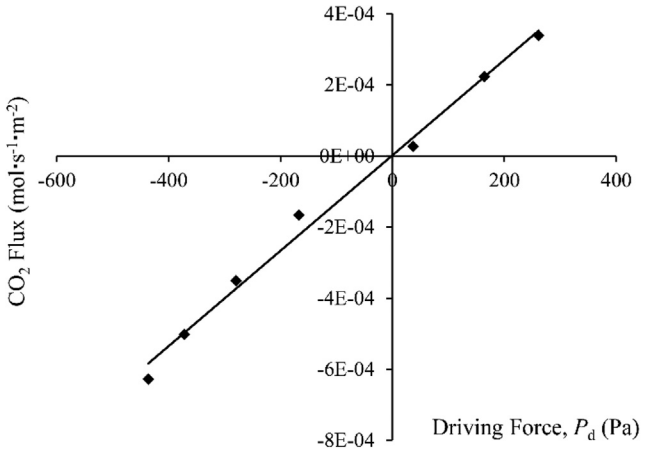

Fig. 2. Measurement of CO_2 absorption in 30% PZ with the WWC at CO_2 equilibrium partial pressure of 510 Pa at 40 °C.

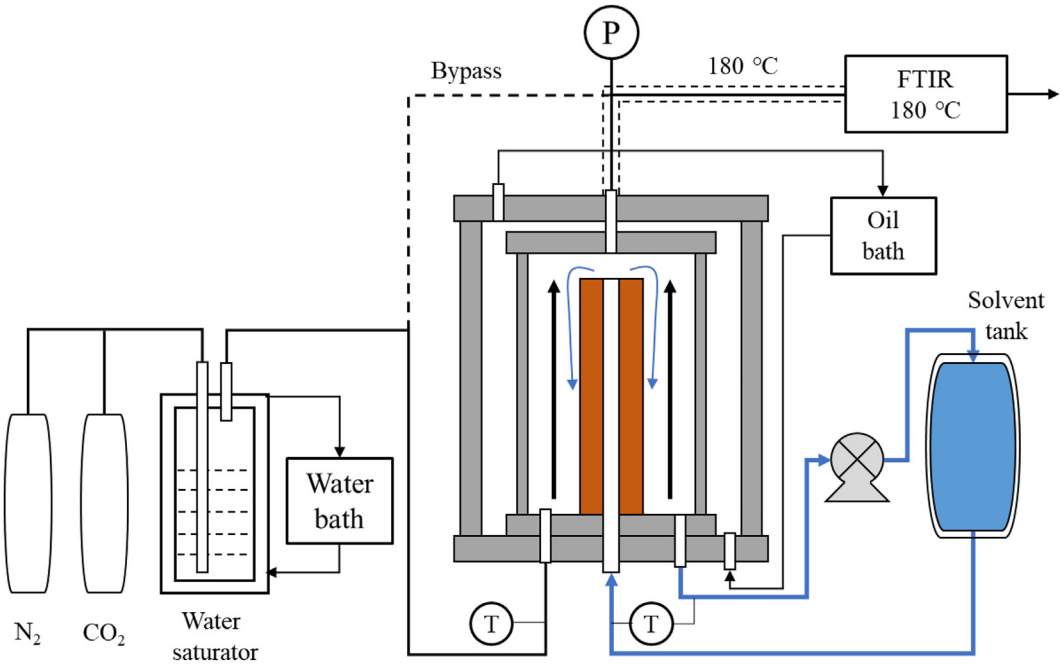

Fig. 1. FTIR coupled wetted wall column (WWC) experimental system.

5 m PZ at CO_2 partial pressure of 510 Pa at 40 °C.

Two-film theory can be used to interpret the mass transfer of CO_2 absorption into amine solution in the WWC [6]. CO_2 first diffuses from the bulk gas phase to the gas film, and the reaction occurs in the liquid film near the interface. The reaction products diffuse from the interface to the bulk liquid phase. The gas and liquid composition in the bulk phase were assumed to be constant, and the influence of absorption flux on the composition of the solution in the system can be neglected because of the large solvent inventory. The total mass transfer coefficient (K_G) is determined by the gas film mass transfer (k_g) and the liquid film mass transfer (k_g') as expressed in Eq. (4).

$$\frac{1}{K_G} = \frac{1}{k_g'} + \frac{1}{k_g} \tag{4}$$

The gas film mass transfer coefficient (k_g) is determined by the geometry of the WWC and the gas flow rate. A previously determined correlation for this WWC [34] is expressed as Eq. (5).

$$Sh = 1.075\left(Re \cdot Sc \cdot \frac{d}{h}\right)^{0.85} \tag{5}$$

Sh, *Re*, and *Sc* are Sherwood, Reynolds, and Schmidt numbers, respectively.

The liquid film mass transfer coefficient (k_g') with a gas phase driving force is determined by the physical liquid film mass transfer coefficient and chemical reaction enhancement, as expressed in Eq. (6).

$$k_g' = \frac{E \cdot k_l^0}{H_{CO_2,soln}} \tag{6}$$

where k_l^0 is the liquid film mass transfer coefficient without reaction, E is chemical reaction enhancement factor, and $H_{CO2,soln}$ is the Henry's law constant of CO_2 in amine solutions. When $E \gg 1$, the chemical reaction rate is much faster than the physical mass transfer rate.

The physical liquid film mass transfer coefficient (k_l^0) is related to liquid flow rate, physical properties of amine solution, and parameters of the WWC. A correlation expressed as Eq. (7) was previously determined for the WWC in this work [35].

$$k_l^0 = \left(\frac{3^{1/3}2^{1/2}}{\pi^{1/2}}\right)\left(\frac{Q_l^{1/3}h^{1/2}W^{2/3}}{A}\right)\left(\frac{\rho g}{\mu}\right)^{1/6} D_{CO_2,soln}^{1/2} \tag{7}$$

where Q_l is liquid flow rate. h and W are the height and perimeter of the WWC, respectively. ρ and μ are the density and viscosity of the amine solution, respectively. $D_{CO2,soln}$ is the diffusion coefficient of CO_2 in amine solution.

The pseudo-first-order (PFO) regime applies to most reactions of CO_2 and amine. With activity-based kinetics, the reaction rate is assumed to be first order with CO_2 activity in amine solutions and k_g' is simplified as Eq. (8).

$$k_g' = \sqrt{\frac{k_1[\text{Amine}]D_{CO_2,soln}}{\gamma_{CO_2}}}\frac{1}{H_{CO_2,water}} \tag{8}$$

k_1 is the pseudo-first-order rate constant. γ_{CO2} is the CO_2 activity coefficient in amine solution, which can be calculated using CO_2 Henry's constant ($H_{CO2,water}$) in water as a reference state by Eq. (9).

$$H_{CO_2,soln} = \gamma_{CO2} H_{CO_2,water} \tag{9}$$

2.4. Physical solubility and diffusion coefficient

The physical solubility of CO_2 in amine solution was calculated using the N_2O analogy method, as follows:

$$H_{CO_2,soln} = H_{N_2O,soln}\left(\frac{H_{CO_2,water}}{H_{N_2O,water}}\right) \tag{10}$$

The Henry's law constant of CO_2 and N_2O in water was measured, as Eq. (11) and (12) [36].

$$H_{CO_2,water} = 2.82 \times 10^6 \exp(-2044/T) \tag{11}$$

$$H_{N_2O,water} = 8.55 \times 10^6 \exp(-2284/T) \tag{12}$$

The CO_2 diffusion coefficient ($D_{CO2,soln}$) in amine solution is dependent on viscosity according to Eq. (13) [36]. $D_{CO2,water}$ was measured as a function of temperature as expressed in Eq. (14).

$$D_{CO_2,soln} = D_{CO_2,water}\left(\frac{\mu_w}{\mu}\right)^{0.8} \tag{13}$$

$$D_{CO_2,water} = 2.35 \times 10^{-6} \exp(-2119/T) \tag{14}$$

Density, viscosity, and Henry's constant in unloaded AEEA and DEEA solutions were obtained from reported data [6,37–42] or interpolated. Density and viscosity of CO_2 loaded amine solutions were assumed to be linear with CO_2 loading (α) as shown in Eqs. (15) and (16).

$$\rho_{loaded} = \rho_{loaded} + k_\rho \cdot \alpha \tag{15}$$

$$\mu_{loaded} = \mu_{loaded} + k_\mu \cdot \alpha \tag{16}$$

where k_ρ and k_μ are the correlated coefficients for density and viscosity of CO_2 loaded amine solutions. Table 3 presents the data sources used in this work to determine the density and viscosity of unloaded and loaded AEEA and DEEA solutions at 40 °C. Density of unloaded AEEA/DEEA blend was calculated as a weighted-average value of the densities of AEEA and DEEA solutions. Viscosity of unloaded AEEA/DEEA blend was measured previously by Liu et al. [15,29]. Since DEEA is less than 20% in the aqueous phase and is more than 81% in the organic phase, k_ρ and k_μ for the loaded aqueous phase are approximated as those of AEEA solution, and k_ρ and k_μ for the loaded organic phase is assumed to be equal to that of DEEA solution. The Henry's constant in CO_2-loaded amine solution was assumed to be equal to that in unloaded amine solution. The Henry's constant in the aqueous phase was approximated as that in the AEEA solution and the Henry's constant in the organic phase was approximated as that in DEEA solution.

3. Results and discussion

3.1. Mass transfer coefficients

The absorption rate and CO_2 equilibrium pressure (P_{CO2}*) of 25% AEEA, 50% DEEA, and AEEA/DEEA blends were measured at various CO_2 loading at 40 °C. The mass transfer coefficients (K_G, k_g, and k_g'), CO_2 equilibrium pressure (P_{CO2}*), and the kinetic parameters are listed in Table 4. The gas side mass transfer coefficient (k_g) is nearly constant at 4.4 × 10^6 mol·m^{-2}·s^{-1}·Pa^{-1} since all experiments described in this paper were run at the same gas flow rate in the same WWC. For CO_2 absorption in fast amine solutions such as unloaded 25% AEEA, the gas

Table 3
Data sources used to determine density, viscosity, and CO_2 physical solubility at 40 °C.

	Amine	T (°C)	Mass fraction	CO_2 loading (mol/mol)	Points	Ref.
Density	AEEA	40	0.05–0.30	0	6	[37]
	DEEA	40	0.05–1.00	0	16	[38]
		40	0.24	0.14–0.79	6	[38]
		40	0.61	0.14–0.42	4	[38]
Viscosity	AEEA	40	0.05–0.30	0	4	[37]
		40	0.05–0.30	0	6	[39]
		40	0.30, 0.40	1.00	2	[29]
	DEEA	40	0.05–1.00	0	15	[40]
		40	0.24	0.14–0.68	6	[40]
		40	0.61	0.09–0.42	7	[40]
$H_{CO2,soln}$	AEEA	30	0.156–0.31	0	4	[41]
		30–50	0.20	0	5	[6]
	DEEA	35	0.12–1.00	0	6	[42]
		45	0.12–1.00	0	6	[42]

Table 4
Mass transfer and kinetic parameters of CO_2 absorption into aqueous 25% AEEA, 50% DEEA, and AEEA/DEEA blends at 40 °C by WWC.[a]

CO_2 [b] (mol/kg)	P_{CO2}* (Pa)	K_G (10^{-6}mol·m^{-2}·s^{-1}·Pa^{-1})	k_g'	ρ (10^3kg/m^3)	μ (mPa·s)	$D_{CO2,soln}$ (10^{-10}m^2/s)	k_l^0 (10^{-5}m/s)	$H_{CO2,soln}$ (10^3Pa·m^3·mol^{-1})	E
25% AEEA									
0	- [c]	2.15	4.16	1.01	1.41	14.6	2.03	4.14	849
0.44	–	1.87	3.23	1.02	1.50	13.8	1.96	4.14	682
1.02	41	1.62	2.56	1.05	1.63	13.0	1.88	4.14	564
1.65	418	0.834	1.03	1.07	1.76	12.2	1.80	4.14	236
2.27	8645	0.232	0.245	1.09	1.90	11.5	1.73	4.14	60
50% DEEA									
0	–	0.368	0.401	0.958	4.20	6.08	1.08	2.96	110
0.39	430	0.219	0.230	0.975	5.72	4.75	0.911	2.96	75
0.85	1450	0.143	0.148	0.995	7.52	3.82	0.783	2.96	57
1.14	3400	0.114	0.117	1.01	8.66	3.41	0.724	2.96	49
1.64	5150	0.096	0.098	1.03	10.6	2.90	0.648	2.96	46
25% AEEA + 50% DEEA									
0	–	2.47	5.57	0.985	6.35	4.37	0.860	2.96	1919
0.36	54	2.35	5.01	1.00	6.43	4.33	0.856	2.96	1734
0.64	90	2.09	3.99	1.01	6.49	4.30	0.854	2.96	1386
42% AEEA + 12% DEEA (aqueous phase 1)									
1.62	23	1.14	1.54	1.04	12.3	2.58	0.597	4.88	1259
2.56	111	0.675	0.796	1.06	19.0	1.82	0.467	4.88	832
3.10	360	0.506	0.527	1.07	24.1	1.50	0.409	4.88	683
3.75	1726	0.281	0.300	1.08	31.7	1.21	0.351	4.88	417
4.29	10,051	0.139	0.143	1.09	39.3	1.02	0.311	4.88	225
10% AEEA + 81% DEEA (organic phase 1)									
0.10	48	3.01	9.35	0.976	7.31	3.91	0.793	1.59	1881
0.28	120	2.33	4.91	1.01	7.96	3.65	0.760	1.59	1031
0.48	293	1.24	1.72	1.05	8.65	3.41	0.729	1.59	376
0.81	1020	0.632	0.737	1.11	9.77	3.10	0.687	1.59	171
1.04	4597	0.341	0.370	1.15	10.53	2.92	0.662	1.59	89
42% AEEA + 15% DEEA (aqueous phase 2)									
2.25	58.9	0.756	0.911	1.05	17.2	1.97	0.494	4.88	900
3.40	608	0.351	0.381	1.07	28.8	1.30	0.370	4.88	502
4.25	7210	0.163	0.169	1.08	40.9	0.986	0.304	4.88	271
4% AEEA + 87% DEEA (organic phase 2)									
0.05	112	1.68	2.70	0.958	6.37	4.36	0.855	1.37	432
0.20	496	0.812	1.00	0.987	6.87	4.10	0.823	1.37	165
0.35	1873	0.459	0.512	1.01	7.34	3.89	0.796	1.37	88
41% AEEA + 18% DEEA (aqueous phase 3)									
0.85	–	2.04	3.78	1.02	9.67	3.12	0.682	4.88	2706
2.49	127	0.617	0.717	1.05	25.8	1.41	0.393	4.88	891
3.38	612	0.440	0.489	1.07	41.8	0.968	0.300	4.88	796
3.82	1592	0.259	0.306	1.08	52.4	0.808	0.264	4.88	565
4.32	7153	0.151	0.156	1.09	66.9	0.664	0.230	4.88	331
2% AEEA + 92% DEEA (organic phase 3)									
0.07	950	0.560	0.641	0.956	5.17	5.15	0.961	1.18	79
0.15	3430	0.351	0.381	0.971	5.43	4.96	0.938	1.18	48
0.24	7130	0.239	0.252	0.987	5.70	4.77	0.915	1.18	32

[a] $k_g = 4.4 \times 10^{-6}$ mol.m^{-2}.s^{-1}.Pa^{-1}.
[b] mol CO_2 /kg (water + amine).
[c] P_{CO2}* is too small to be measured by the WWC.

side mass transfer resistance ($1/k_g$) accounts for 48% of the total mass transfer resistance ($1/K_G$). The gas side mass transfer resistance ($1/k_g$) accounts for only 8% of the rate in unloaded 50% DEEA. The liquid mass transfer coefficient (k_g') was used to represent the CO_2 absorption rate of amine solutions in this work.

3.2. CO_2 absorption rate (k_g') of single amine solutions

The CO_2 absorption rate (k_g') and CO_2 equilibrium pressure (P_{CO2}*) of 25% AEEA and 50% DEEA at 40 °C are given in Table 4. Fig. 3 shows that P_{CO2}* of 25% AEEA by the WWC agrees well with the VLE data of 15% AEEA reported by Guo et al. [43] and those of 30% AEEA reported by Ma'mum et al. [44], which demonstrated the reliability of P_{CO2}* obtained in this work. Fig. 4 suggests that P_{CO2}* of 50% DEEA by the WWC is in good agreement with the VLE data of 52% DEEA reported by Luo et al. [45]. In combination with the data of Monteiro et al. [46] and those of Luo et al. [45] in 68 and 25 wt% it appears that P_{CO2} increases with DEEA. This behavior is consistent with a decrease in solution

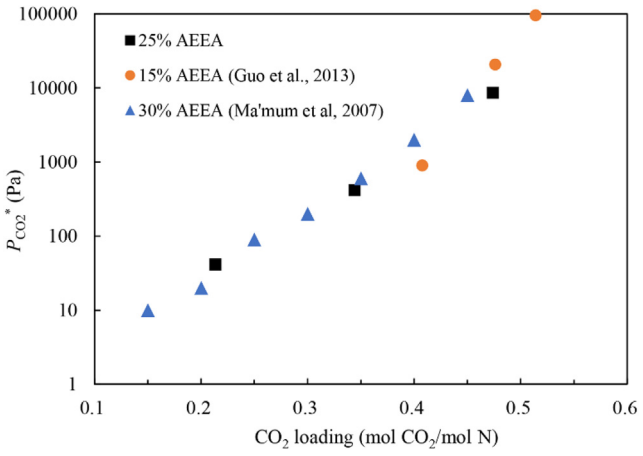

Fig. 3. P_{CO2}* of 25% AEEA at 40 °C by WWC compared to the VLE data from equilibrium apparatus.

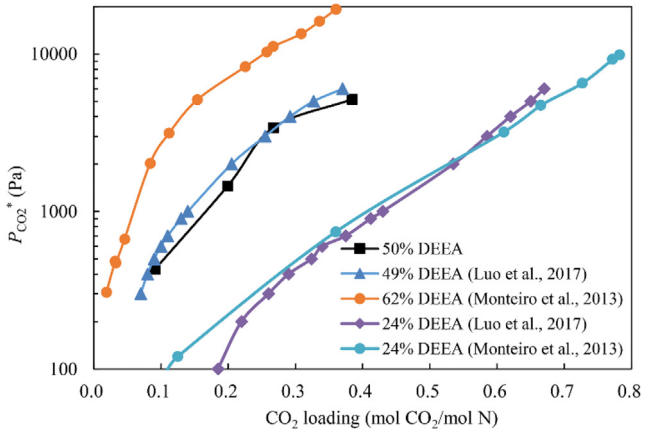

Fig. 4. P_{CO2}* of 50% DEEA at 40 °C by WWC compared to VLE data from equilibrium apparatus.

polarity with a greater concentration of the less polar DEEA.

Amine solvent in a typical absorber at 40 °C has a lean loading with P_{CO2}* of 100 to 500 Pa and a rich loading with P_{CO2}* of 1000 to 5000 Pa. For a fair comparison with 30% MEA and 30% PZ (data from Dugas [35]), the k_g' of 25% AEEA and 50% DEEA is plotted against P_{CO2}* from 100 to 10000 Pa in Fig. 5. The k_g' decreases in the order of 30% PZ, 25% AEEA, 25% MEA, and 50% DEEA. DEEA is a less reactive tertiary amine so its k_g' is 1–2 orders of magnitude smaller than those of 25% AEEA, 30% MEA, and 30% PZ. The chemical reaction enhancement factor (E) of 50% DEEA is about 7 times lower than that of 25% AEEA.

3.3. CO_2 absorption rate (k_g') of AEEA/DEEA

The k_g' and P_{CO2}* of the biphasic solvent 25% AEEA/50% DEEA with various CO_2 loadings at 40 °C are given Table 4. 25% AEEA/50% DEEA is homogeneous at 0 to 0.64 mol CO_2/kg (amine + water). At increased CO_2 loading, the biphasic solvent forms aqueous and organic phases (Table 2). The k_g' and P_{CO2}* of the aqueous and organic phases at various CO_2 loading at 40 °C are given in Table 4. Fig. 6 plots k_g' of single amine solutions and AEEA/DEEA blends with variable CO_2 loading against P_{CO2}* from 10 to 10000 Pa at 40 °C. The data for 30% MEA and 30% PZ are taken from Dugas [35]. There are only two data points for 25% AEEA/50% DEEA because two phases are formed when P_{CO2}* is greater than 100 Pa.

As shown in Fig. 6, the k_g' of the organic phases is over 2 times greater than that of the aqueous phases. This is due to the greater liquid film mass transfer coefficient (k_l^0) and greater physical solubility ($1/H_{CO2,soln}$) of CO_2 in the organic phases. The estimated k_l^0 and ($1/H_{CO2,soln}$) of different amine solutions is plotted against P_{CO2}* in Fig. 7 and Fig. 8. The organic phases have a 2–3 times greater physical mass transfer coefficient (k_l^0) and 3–4 times greater CO_2 physical solubility ($1/H_{CO2,soln}$) than the aqueous phases. According to the definition of k_l^0 by Eq. (7) and the relation of $D_{CO2,soln}$ by Eq. (13), $k_l^0 \propto \mu^{-0.567}$, which suggests that a lower viscosity results in a greater liquid film mass transfer coefficient. As shown in Table 4, 25% AEEA has the lowest viscosity and greatest k_l^0. 50% DEEA has a similar viscosity to the organic phases and therefore their k_l^0 are very similar. The concentrated aqueous phases of the biphasic blend have the greatest viscosity and smallest k_l^0.

The rate behavior of the three aqueous phases in Fig. 6 is practically identical because their compositions are practically the same. As shown in Table 1, the concentration of the kinetically active species, AEEA, only varies from 41 to 42 wt%.

Fig. 9 shows the chemical enhancement factor (E) of CO_2 absorption

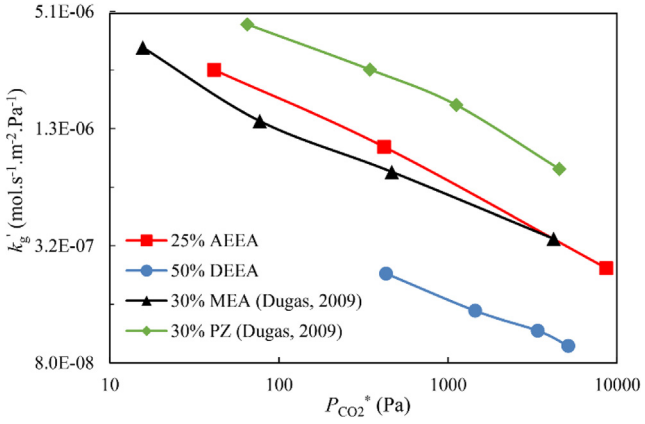

Fig. 5. k_g' of 25% AEEA and 50% DEEA at 40 °C by WWC.

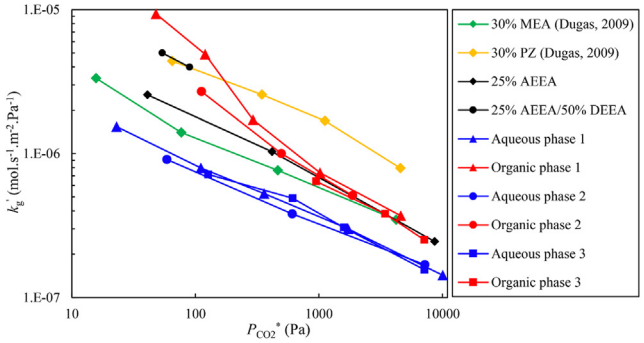

Fig. 6. k_g' of AEEA/DEEA blends at 40 °C by WWC.

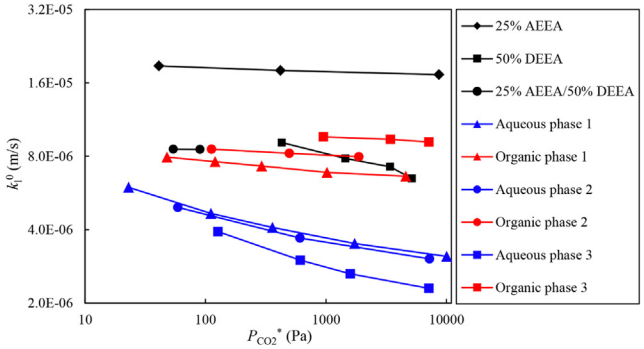

Fig. 7. Physical liquid film mass transfer coefficient (k_l^0) of CO_2 absorption in different amine solutions in WWC at 40 °C.

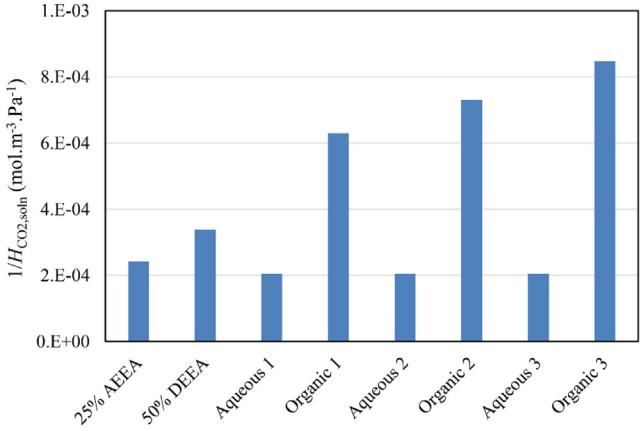

Fig. 8. Physical solubility ($1/H_{CO2,soln}$) of CO_2 in different amine solutions in WWC at 40 °C.

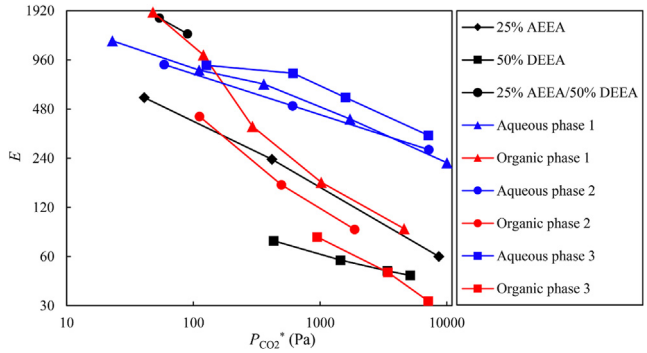

Fig. 9. Chemical enhancement factor (E) of CO_2 absorption in different amine solutions in WWC at 40 °C.

in different amine solutions. The E is far greater than 1 which suggests that the absorption rate (k_g') of aqueous amine solutions is dominated by the chemical enhancement. As P_{CO2}* increases, E decreases because free amine decreases as more CO_2 is absorbed into the solution. In the aqueous phase E is 2–10 times greater than in the organic phase at P_{CO2}* greater than 100 Pa. The kinetic reaction rate constant of CO_2 with AEEA is two orders of magnitude greater than that of DEEA [20]. Fig. 9 also suggests E in 25% AEEA is 3 times greater than that in 50% DEEA. According to Table 2, AEEA is rich in aqueous phase and lean in organic phase. In the P_{CO2}* range of 10 to 100 Pa, the E of 25% AEEA/50% DEEA and organic phase 1 (10% AEEA/81% DEEA) are greater than that of aqueous phase. It may be that Henry's constant of CO_2 physical solubility in 25% AEEA/50% DEEA and 10% AEEA/81% DEEA is inaccurate as it was estimated as the same $H_{CO2,soln}$ as in 50% DEEA and 81% DEEA.

25% AEEA has a 2 times smaller E than aqueous phase as shown in Fig. 9 but shows a 2–3 times faster CO_2 absorption rate (k_g') as shown in Fig. 6. This is because 25% AEEA has greater physical CO_2 solubility ($1/H_{CO2,soln}$) and physical mass transfer coefficient (k_l^0) at the same CO_2 equilibrium partial pressure. As shown in Figs. 7 and 8, k_l^0 in 25% AEEA is 3–6 times greater than in aqueous phase, and $1/H_{CO2,soln}$ of 25% AEEA is 20% higher than those of aqueous phases.

3.4. CO_2 capacity

Fig. 10 gives P_{CO2}* of the single amine solutions and AEEA/DEEA blends as a function of CO_2 loading at 40 °C. The aqueous phase has a larger CO_2 loading than the single amine solutions and organic phase at the same P_{CO2}*. This is due to the greater chemical CO_2 solubility in aqueous phases. Compared to single amine solutions such as 30% MEA, 30% PZ and 25% AEEA, the aqueous phase is rich in concentrated reactive amine (40–42% AEEA). As the reactive amine concentration increases, CO_2 solubility in amine solution increases at the same CO_2 partial pressure and temperature [47]. The organic phase has the lowest

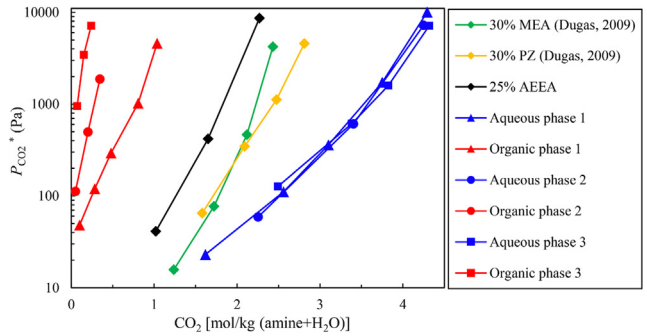

Fig. 10. Total CO_2 solubility in the aqueous and organic phases at 40 °C by WWC.

CO_2 loading compared to the aqueous phase and single amine solutions. The DEEA in the organic phase is more than 80 wt% and the physical CO_2 solubility in the organic phase is 3–4 times greater than that of single amine and aqueous phases as shown in Fig. 8.

Table 5 compares the CO_2 capacity of different amine solutions at the same mass transfer driving force in the absorber. The CO_2 capacity is defined as the difference between rich loading and lean loading. In the case of gas turbine flue gas with 3% CO_2 by volume, the lean and rich loadings correspond to P_{CO2}* of 100 Pa and 1000 Pa at 40 °C at 90% CO_2 removal. In the case of coal flue gas with 12% CO_2 by volume, the lean and rich loadings correspond to P_{CO2}* of 500 Pa and 5000 Pa at 40 °C at 90% CO_2 removal. The CO_2 capacity with gas turbine is generally greater than with coal flue gas. With the gas turbine case as an example, the CO_2 capacity of 25% AEEA is 32% greater than that of 30% MEA and 19% lower than that of 30% PZ. The CO_2 capacity of the aqueous phase is 44% to 76% greater than that of 30% PZ. However, the organic phase has a 7% to 86% lower CO_2 capacity than that of 30% MEA. The k_g' at lean and rich conditions was estimated according to Fig. 6 and presented in Table 5. The k_g' of the organic phase is much greater than that of 30% MEA at lean and rich loading and is even greater than that of 30% PZ at lean loading.

3.5. CO_2 absorption rate (k_g') in biphasic region

Based on Fig. 6 and Fig. 10, the P_{CO2}* and k_g' of the aqueous and organic phases at the specific CO_2 loading listed in Table 2 was interpolated. For example, when the total loading of 25% AEEA/50% DEEA is 1.10 mol/kg (amine + H_2O), the aqueous phase with CO_2 loading of 2.59 mol/kg has a P_{CO2}* of 130 Pa while the organic phase with CO_2 loading of 0.13 mol/kg has a P_{CO2}* of 59 Pa. The disagreement of the P_{CO2}* between the aqueous and organic phases might be due to the large uncertainty of CO_2 loading in the organic phase. In the previous work, the CO_2 loading was measured using an acid-base titration method [29], which was originally designed to determine CO_2 loading of 30% MEA (0.1–0.5 mol CO_2/mol MEA). The measurement error may be greater for extreme low CO_2 loading of the organic phase.

The CO_2 loading of the aqueous phase was used to estimate the P_{CO2}* in the biphasic region. It is assumed that the organic phase has the same P_{CO2}* as the aqueous phase. The k_g' of the aqueous and organic phases was then interpolated, as shown in Fig. 11. The data in hollow and dashed lines indicate the estimated k_g' of 25% AEEA/50% DEEA in the biphasic region. The organic phase has a faster k_g' than the aqueous phase and than single amine solutions such as 30% MEA and 25% AEEA. The k_g' of the organic phase is greater than 30% PZ at P_{CO2}* lower than 200 Pa which is a typical lean loading condition. It would be advantageous if the organic phase contacts the gas phase and absorbs CO_2 in the absorber when the biphasic solvent is used for CO_2 capture. Previous NMR analysis [29] indicated that CO_2 products (AEEA carbamates and bicarbonate), pronated AEEA and pronated DEEA were rich in the aqueous phase, while unreacted DEEA and AEEA were concentrated in organic phase. As more CO_2 is absorbed, CO_2 products concentration in aqueous phase are increasing while AEEA concentration in the organic phase is decreasing. In practical absorber, the flow regime of the mixture may be affected by many factors, such as the gas–liquid ratio, the hydrophilic property. It is possible that the mixtures presents two-phase flow in the absorber, and the organic phase would contact with the gas phase because the organic phase is less hydrophilic than the aqueous phase. Experimental verification on this hypothesis is needed in the future study. It is possible that CO_2 was first absorbed by the organic phase and then the reaction products migrated to the aqueous phase. The CO_2 products transfer from the organic phase to aqueous phase is accomplished while the two-phase separation. In the biphasic process, the absorber bottom and the two-phase splitter provide enough resident time for phase separation.

Table 5
CO_2 capacity, k_g' at lean and rich conditions of different amine solutions at 40 °C.

Amines	Loading range (100–1000 Pa)			Loading range (500–5000 Pa)		
	CO_2 capacity	k_g', lean	k_g', rich	CO_2 capacity	k_g', lean	k_g', rich
	mol/kg(amine + H_2O)	mol.m^{-2}.s^{-1}.Pa^{-1}		mol/kg(amine + H_2O)	mol.m^{-2}.s^{-1}.Pa^{-1}	
30% MEA	0.44	1.3E−06	5.8E−07	0.32	7.5E−07	3.2E−07
30% PZ	0.72	3.8E−06	1.8E−06	0.62	2.2E−06	7.5E−07
25% AEEA	0.58	1.8E−06	7.0E−07	0.48	9.5E−07	3.3E−07
Aqueous 1	1.04	7.7E−07	3.8E−07	0.85	4.6E−07	1.9E−07
Organic 1	0.54	5.6E−06	8.3E−07	0.43	1.3E−06	3.7E−07
Aqueous 2	1.07	7.4E−07	3.2E−07	0.83	4.1E−07	1.9E−07
Organic 2	0.24	3.0E−06	7.4E−07	0.25	1.0E−06	3.5E−07
Aqueous 3	1.27	8.3E−07	3.6E−07	0.90	5.1E−07	1.9E−07
Organic 3	0.08	1.9E−06	6.5E−07	0.15	9.0E−07	3.2E−07

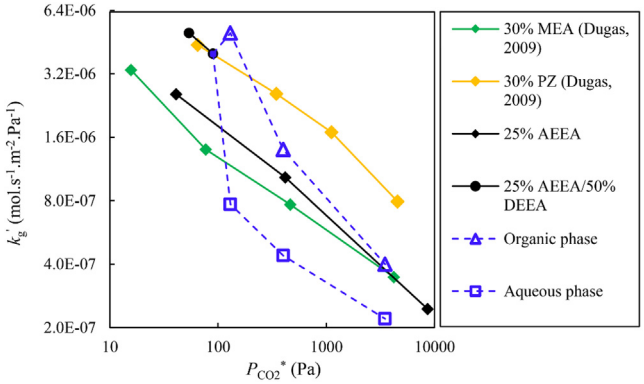

Fig. 11. Estimated k_g' in biphasic region of 25% AEEA/50% DEEA at 40 °C.

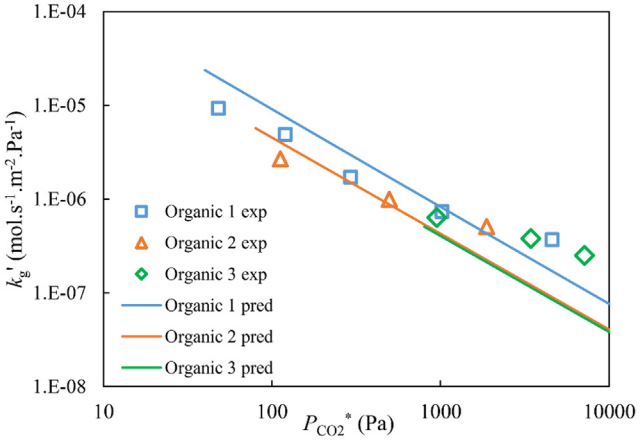

Fig. 12. Predicted k_g' according to the instantaneous reaction mechanism.

3.6. Instantaneous reaction mechanism

As shown in Fig. 6, the k_g' of the organic phase is high at P_{CO2}* lower than 300 Pa, decreases rapidly as P_{CO2}* increases, and is almost identical to that of 30%MEA and 25%AEEA at P_{CO2}* greater than 2000 Pa. The instantaneous reaction mechanism may apply to CO_2 absorption in the organic phase. According to the instantaneous reaction mechanism, the physical diffusion of the products from the gas–liquid interface to bulk liquid dominates the mass transfer resistance in the liquid film [35]. The k_g' can be expressed as:

$$k_g' = k_{l,prod}^0 \frac{d[CO_2]}{dP_{CO2}^*} = k_l^0 \left(\frac{D_{prod,soln}}{D_{CO2,soln}}\right)^{0.5} \frac{d[CO_2]}{dP_{CO2}^*} \quad (17)$$

The physical mass transfer coefficient of the products ($k^0_{l,prod}$) is positively correlated with the square root of the product diffusion coefficient ($D_{prod,soln}$) in amine solution, which is assumed to be a fraction of $D_{CO2,soln}$. The derivative of total dissolved CO_2 ($[CO_2]_T$) with respect to P_{CO2}* is obtained from the VLE curve (Fig. 10). The predicted k_g' of the organic phase according to the instantaneous reaction mechanism is shown in Fig. 12. $D_{prod,soln}/D_{CO2,soln}$ is assumed to be 0.25. The instantaneous reaction mechanism fits the kinetics of CO_2 absorption in the organic phase at P_{CO2}* lower than 1000 Pa. The average relative error between the predicted and experimental k_g' is 27% at P_{CO2}* lower than 1000 Pa. At P_{CO2}* greater than 1000 Pa the measured k_g' is substantially greater than the predicted value. The accuracy of the predictions may be poor at greater P_{CO2}* because of weak assumptions for the properties. The viscosity of the organic phase is assumed to be that of DEEA solutions. The $d[CO_2]_T/dP_{CO2}$* may have large error because the VLE data are sparse as shown in Fig. 10. Dugas [35] reported MEA products diffusion coefficient in 30% MEA and the value of $D_{MEA,prod}/D_{CO2}$ is 0.4 at 40 °C. The value is comparable to the value obtained in this work. The $D_{AEEA,prod}$ is lower than $D_{MEA,prod}$. This is due to the larger molecular size of AEEA. A larger molecular size results in a smaller diffusion coefficient.

4. Conclusions

- Biphasic solvent of 25% AEEA/50% DEEA could be a potential solution for CO_2 capture as it can achieve significant reduction in regeneration energy and have fast CO_2 absorption rate. At CO_2 equilibrium partial pressure (P_{CO2}*) lower than 100 Pa, the CO_2 absorption rate (k_g') of 25% AEEA/50% DEEA is as fast as 30% PZ (3 times faster than 30% MEA).
- In the biphasic region of 25% AEEA/50% DEEA, the CO_2 absorption rate (k_g') of the organic phase is 2–7 times faster than that of the aqueous phase because of greater physical CO_2 solubility and a greater liquid film mass transfer coefficient, which may provide an important reference for researchers in the field of biphasic solvents.
- The CO_2 absorption rate (k_g') of the organic phase decreases faster with increasing equilibrium CO_2 partial pressure (and CO_2 loading) than the aqueous phase as the increase of physical CO_2 solubility is not as great at greater loading.
- The instantaneous reaction mechanism may fit the kinetics of CO_2 absorption in the organic phase.
- If the organic phase determines the rate of CO_2 absorption in the absorber, 25% AEEA/50% DEEA will be faster than 25% AEEA and 30% MEA and competitive with 30% PZ.
- The aqueous phase has a much greater CO_2 capacity than the organic phase. The CO_2 capacity of the aqueous phase is 76% greater than that of 30% PZ, but its viscosity is greater.

Declaration of Competing Interest

The authors declare that they have no known competing financial interests or personal relationships that could have appeared to influence the work reported in this paper.

Acknowledgements

This work was supported by National Natural Science Foundation (No. 51776182). This work was performed at The University of Texas at Austin with financial support from the Texas Carbon Management Program. Fei Liu was supported by the China Scholarship Council (CSC) during his study at The University of Texas at Austin.

References

[1] G.T. Rochelle, Amine Scrubbing for CO_2 Capture, Science 325 (5948) (2009) 1652–1654, https://doi.org/10.1126/science:1176731 https://www.sciencemag.org/lookup/doi/10.1126/science:1176731.
[2] P. Luis, Use of monoethanolamine (MEA) for CO_2 capture in a global scenario: consequences and alternatives, Desalination 380 (2016) 93–99, https://doi.org/10.1016/j.desal.2015.08.004.
[3] K. Li, W. Leigh, P. Feron, H. Yu, M. Tade, Systematic study of aqueous monoethanolamine (MEA)-based CO_2 capture process: techno-economic assessment of the MEA process and its improvements, Appl. Energy 165 (2016) 648–659, https://doi.org/10.1016/j.apenergy.2015.12.109.
[4] P. Frailie, Modeling of carbon dioxide absorption/stripping by aqueous methyldiethanolamine/piperazine (Ph.D. dissertation), The University of Texas at Austin, 2014.
[5] Y. Du, Y. Wang, G.T. Rochelle, Piperazine/4-hydroxy-1-methylpiperidine for CO_2 capture, Chem. Eng. J. 307 (2017) 258–263.
[6] T. Wang, F. Liu, K. Ge, M. Fang, Reaction kinetics of carbon dioxide absorption in aqueous solutions of piperazine, N-(2-aminoethyl) ethanolamine and their blends, Chem. Eng. J. 314 (2017) 123–131.
[7] G. Rochelle, E. Chen, S. Freeman, D. Van Wagener, Q. Xu, A. Voice, Aqueous piperazine as the new standard for CO_2 capture technology, Chem. Eng. J. 171 (2011) 725–733, https://doi.org/10.1016/j.cej.2011.02.011.
[8] S. Zhang, Y. Shen, L. Wang, J. Chen, Y. Lu, Phase change solvents for post-combustion CO_2 capture: Principle, advances, and challenges, Appl. Energy 239 (2019) 876–897, https://doi.org/10.1016/j.apenergy.2019.01.242.
[9] J. Zhang, R. Misch, Y. Tan, D.W. Agar, Novel thermomorphic biphasic amine solvents for CO_2 absorption and low-temperature extractive regeneration, Chem. Eng. Technol. 34 (2011) 1481–1489, https://doi.org/10.1002/ceat.201100099.
[10] J. Zhang, Y. Qiao, W. Wang, R. Misch, K. Hussain, D.W. Agar, Development of an energy-efficient CO_2 capture process using thermomorphic biphasic solvents, Energy Proc. 37 (2013) 1254–1261, https://doi.org/10.1016/j.egypro.2013.05.224.
[11] D.D.D. Pinto, H. Knuutila, G. Fytianos, G. Haugen, T. Mejdell, H.F. Svendsen, CO_2 post combustion capture with a phase change solvent. Pilot plant campaign, Int. J. Greenh. Gas Control. 31 (2014) 153–164, https://doi.org/10.1016/j.ijggc.2014.10.007.
[12] D.D.D. Pinto, S.A.H. Zaidy, A. Hartono, H.F. Svendsen, Evaluation of a phase change solvent for CO_2 capture: absorption and desorption tests, Int. J. Greenh. Gas Control. 28 (2014) 318–327, https://doi.org/10.1016/j.ijggc.2014.07.002.
[13] A.F. Ciftja, A. Hartono, H.F. Svendsen, Experimental study on phase change solvents in CO_2 capture by NMR spectroscopy, Chem. Eng. Sci. 102 (2013) 378–386, https://doi.org/10.1016/j.ces.2013.08.036.
[14] Z. Xu, S. Wang, C. Chen, CO_2 absorption by biphasic solvents: mixtures of 1,4-Butanediamine and 2-(Diethylamino)-ethanol, Int. J. Greenh. Gas Control. 16 (2013) 107–115, https://doi.org/10.1016/j.ijggc.2013.03.013.
[15] F. Liu, M. Fang, N. Yi, T. Wang, Q. Wang, Biphasic behaviors and regeneration energy of a 2-(diethylamino)-ethanol and 2-((2-aminoethyl)amino) ethanol blend for CO_2 capture, Sustain. Energy Fuels. 3 (2019) 3594–3602, https://doi.org/10.1039/c9se00821g.
[16] S. Zhang, Y. Shen, P. Shao, J. Chen, L. Wang, Kinetics, thermodynamics, and mechanism of a novel biphasic solvent for CO_2 capture from flue gas, Environ. Sci. Technol. 52 (2018) 3660–3668, https://doi.org/10.1021/acs.est.7b05936.
[17] B. Lv, X. Zhou, Z. Zhou, G. Jing, Kinetics and thermodynamics of CO_2 absorption into a novel DETA-AMP-PMDETA biphasic solvent, ACS Sustain. Chem. Eng. 7 (2019) 13400–13410, https://doi.org/10.1021/acssuschemeng.9b02700.
[18] W. Conway, Y. Beyad, M. Maeder, R. Burns, P. Feron, G. Puxty, CO_2 absorption into aqueous solutions containing 3-piperidinemethanol: CO_2 mass transfer, stopped-flow kinetics, $^1H/^{13}C$ NMR, and vapor-liquid equilibrium investigations, Ind. Eng. Chem. Res. 53 (2014) 16715–16724.
[19] L. Wang, S. An, Q. Li, S. Yu, S. Wu, Phase change behavior and kinetics of CO_2 absorption into DMBA/DEEA solution in a wetted-wall column, Chem. Eng. J. 314 (2017) 681–687.
[20] E. Kruszczak, H. Kierzkowska-Pawlak, CO_2 capture by absorption in activated aqueous solutions of N, N-diethylethanoloamine, Ecol. Chem. Eng. S 24 (2017) 239–248, https://doi.org/10.1515/eces-2017-0016.
[21] Z. Xu, S. Wang, C. Chen, Kinetics study on CO_2 absorption with aqueous solutions of 1,4-butanediamine, 2-(diethylamino)-ethanol, and their mixtures, Ind. Eng. Chem. Res. 52 (2013) 9790–9802, https://doi.org/10.1021/ie4012936.
[22] B. Yu, H. Yu, K. Li, Q. Yang, R. Zhang, L. Li, Z. Chen, Characterisation and kinetic study of carbon dioxide absorption by an aqueous diamine solution, Appl. Energy 208 (2017) 1308–1317, https://doi.org/10.1016/j.apenergy.2017.09.023.
[23] H. Gao, B. Xu, H. Liu, Z. Liang, Effect of amine activators on aqueous N, N-diethylethanolamine solution for postcombustion C_O2 capture, Energy Fuels 30 (2016) 7481–7488, https://doi.org/10.1021/acs.energyfuels.6b00671.
[24] J.G.M. Monteiro, H. Majeed, H. Knuutila, H.F. Svendsen, Kinetics of CO_2 absorption in aqueous blends of N, N-diethylethanolamine (DEEA) and N-methyl-1,3-propanediamine (MAPA), Chem. Eng. Sci. 129 (2015) 145–155, https://doi.org/10.1016/j.ces.2015.02.001.
[25] U. Liebenthal, D.D.D. Pinto, M.S. Monteiro, H.F. Svendsen, A. Kather, Overall process analysis and optimisation for CO_2 capture from coal fired power plants based on phase change solvents forming two liquid phases, Energy Proc. 37 (2013) 1844–1854.
[26] H. Kierzkowska-pawlak, Kinetics of CO_2 absorption in aqueous N, N-diethylethanolamine and its blend with N-(2-aminoethyl) ethanolamine using a stirred cell reactor, Int. J. Greenh. Gas Control. 37 (2015) 76–84, https://doi.org/10.1016/j.ijggc.2015.03.002.
[27] L. Li, Carbon Dioxide Solubility and Mass Transfer in Aqueous Amines for Carbon Capture, The University of Texas at Austin, 2015.
[28] L. Wang, S. An, S. Yu, S. Zhang, Y. Zhang, M. Li, Q. Li, Mass transfer characteristics of CO_2 absorption into a phase-change solvent in a wetted-wall column, Int. J. Greenh. Gas Control. 64 (2017) 276–283, https://doi.org/10.1016/j.ijggc.2017.08.001.
[29] F. Liu, M. Fang, W. Dong, T. Wang, Z. Xia, Q. Wang, Z. Luo, Carbon dioxide absorption in aqueous alkanolamine blends for biphasic solvents screening and evaluation, Appl. Energy 233–234 (2019) 468–477, https://doi.org/10.1016/j.apenergy.2018.10.007.
[30] X. Chen, G.T. Rochelle, Aqueous piperazine derivatives for CO_2 capture: Accurate screening by a wetted wall column, Chem. Eng. Res. Des. 89 (2011) 1693–1710, https://doi.org/10.1016/j.cherd.2011.04.002.
[31] L. Li, A.K. Voice, H. Li, O. Namjoshi, T. Nguyen, Y. Du, G.T. Rochelle, Amine blends using concentrated piperazine, Energy Procedia 37 (2013) 353–369, https://doi.org/10.1016/j.egypro.2013.05.121.
[32] Y. Du, Y. Yuan, G.T. Rochelle, Capacity and absorption rate of tertiary and hindered amines blended with piperazine for CO_2 capture, Chem. Eng. Sci. 155 (2016) 397–404, https://doi.org/10.1016/j.ces.2016.08.017.
[33] Y. Yuan, G.T. Rochelle, CO_2 absorption rate in semi-aqueous monoethanolamine, Chem. Eng. Sci. 182 (2018) 56–66, https://doi.org/10.1016/j.ces.2018.02.026.
[34] S. Bishnoi, G.T. Rochelle, Absorption of carbon dioxide into aqueous piperazine: reaction kinetics, mass transfer and solubility, Chem. Eng. Sci. 55 (2000) 5531–5543, https://doi.org/10.1016/S0009-2509(00)00182-2.
[35] R.E. Dugas, Carbon Dioxide Absorption, Desorption, and Diffusion in Aqueous Piperazine and Monoethanolamine, The University of Texas at Austin, 2009.
[36] G.F. Versteeg, W.P.M. van Swaal, Solubility and Diffusivity of Acid Gases (CO_2, N_2O) in Aqueous Alkanolamine Solutions, J. Chem. Eng. Data 33 (1988) 29–34, https://doi.org/10.1021/je00051a011.
[37] S. Mukherjee, A.N. Samanta, Kinetic study of CO_2 absorption in aqueous solutions of 2-((2-aminoethyl)amino)-ethanol using a stirred cell reaction calorimeter, Int. J. Chem. Kinet. 51 (2019) 943–957, https://doi.org/10.1002/kin.21322.
[38] D.D.D. Pinto, J.G.M.S. Monteiro, B. Johnsen, H.F. Svendsen, H. Knuutila, Density measurements and modelling of loaded and unloaded aqueous solutions of MDEA (N-methyldiethanolamine), DMEA (N, N-dimethylethanolamine), DEEA (diethylethanolamine) and MAPA (N-methyl-1,3-diaminopropane), Int. J. Greenh. Gas Control. 25 (2014) 173–185, https://doi.org/10.1016/j.ijggc.2014.04.017.
[39] D. Pandey, M.K. Mondal, Experimental data and modeling for viscosity and refractive index of aqueous mixtures with 2-(methylamino)ethanol (MAE) and aminoethylethanolamine (AEEA), J. Chem. Eng. Data 64 (2019) 3346–3355, https://doi.org/10.1021/acs.jced.9b00171.
[40] D.D.D. Pinto, B. Johnsen, M. Awais, H.F. Svendsen, H.K. Knuutila, Viscosity measurements and modeling of loaded and unloaded aqueous solutions of MDEA, DMEA, DEEA and MAPA, Chem. Eng. Sci. 171 (2017) 340–350.
[41] A.B. Bindwal, P.D. Vaidya, E.Y. Kenig, Kinetics of carbon dioxide removal by aqueous diamines, Chem. Eng. J. 169 (2011) 144–150, https://doi.org/10.1016/j.cej.2011.02.074.
[42] J.G.M.S. Monteiro, H. Knuutila, N.J.M.C. Penders-van Elk, G. Versteeg, H.F. Svendsen, Kinetics of CO_2 absorption by aqueous N, N-diethylethanolamine solutions: literature review, experimental results and modelling, Chem. Eng. Sci. 127 (2015) 1–12, https://doi.org/10.1016/j.ces.2014.12.061.
[43] C. Guo, S. Chen, Y. Zhang, Solubility of carbon dioxide in aqueous 2-(2-aminoethylamine)ethanol (AEEA) solution and its mixtures with N-methyldiethanolamine/2-amino-2-methyl-1-propanol, J. Chem. Eng. Data 58 (2013) 460–466, https://doi.org/10.1021/je301174v.
[44] S. Ma'mun, H.F. Svendsen, K.A. Hoff, O. Juliussen, Selection of new absorbents for carbon dioxide capture, Energy Convers. Manage. 48 (2007) 251–258, https://doi.org/10.1016/j.enconman.2006.04.007.
[45] X. Luo, N. Chen, S. Liu, H. Zhang, R.O. Idem, P. Tontiwachwuthikul, Z. Liang, Experiments and modeling of vapor-liquid equilibrium in DEEA-CO_2-H_2O system, Energy Proc. 114 (2017) 1530–1537, https://doi.org/10.1016/j.egypro.2017.03.1283.
[46] J.G.M.S. Monteiro, D.D.D. Pinto, S.A.H. Zaidy, A. Hartono, H.F. Svendsen, VLE data and modelling of aqueous N, N-diethylethanolamine (DEEA) solutions, Int. J. Greenh. Gas Control. 19 (2013) 432–440, https://doi.org/10.1016/j.ijggc.2013.10.001.
[47] U.E. Aronu, S. Gondal, E.T. Hessen, T. Haug-Warberg, A. Hartono, K.A. Hoff, H.F. Svendsen, Solubility of CO_2 in 15, 30, 45 and 60 mass% MEA from 40 to 120 °C and model representation using the extended UNIQUAC framework, Chem. Eng. Sci. 66 (2011) 6393–6406, https://doi.org/10.1016/j.ces.2011.08.042.